United Technologies Research Center

TITLE:	Plasma-assisted Combustor Dynamics Control
TYPE OF REPORT:	Summary of Research
PRINCIPAL INVESTIGATOR:	Wookyung Kim
PERIOD:	11/15/2012 – 2/14/2014
INSTITUTION:	United Technologies Research Center 411 Silver Lane East Hartford, CT 06108
GRANT NUMBER:	NNX13AB89A
TECHNICAL CONTACT:	Dr. Wookyung Kim Phone: (860) 610-7266 Fax: 860-998-3521 Email: kimw@utrc.utc.com
BUSINESS CONTACT:	Mr. James Bickford Phone: (860) 610-7285 Fax: (860) 998-3521 Email: BickfoJL@utrc.utc.com
DATE SUBMITTED:	May 13, 2014

TABLE OF CONTENTS

1. Executive Summary

The primary purpose of the current research is to demonstrate and interpret the effectiveness of implementing a plasma discharge to improve combustor dynamics and flame stability. Specifically, a nano-second pulsed plasma discharge (NSPD) was applied to a premixed methane/air dump combustor for mitigation of dynamic combustion instabilities with a minimal NO_X penalty. As a result, up to ~ 25 dB noise reduction was observed in the presence of the NSPD. High speed imaging suggests that the NSPD relocated the flame stabilization point from the outer recirculation zone to the center zone. Due to the highly non-equilibrium temperature characteristic of the NSPD, the incremental increase of emissions in the presence of the discharge was minimal, typically around 0.5 $EINO_X$, while the increase of combustion efficiency could be significant and on the order of ~ 10%. A new control algorithm that measured pressure oscillation amplitude, and actuated with plasma power was developed. This algorithm does not require knowledge/measurement of pressure oscillation phase, and therefore, avoids challenges associated with convective and actuator phase delays. The impact of NSPD on swirl-stabilized flames was also investigated for swirl numbers from 0 – 0.33. It is shown that the relative effect of NSPD for dynamics reduction decreases with increasing swirl due to the inherent decrease in nascent flame dynamics. All observations in the current work suggest that the flame shape plays a central role in determining the degree of plasma effectiveness and that any noisy, outer recirculation zone stabilized flames will be significantly improved by this implementation of NSPD.

2. Experimental Details

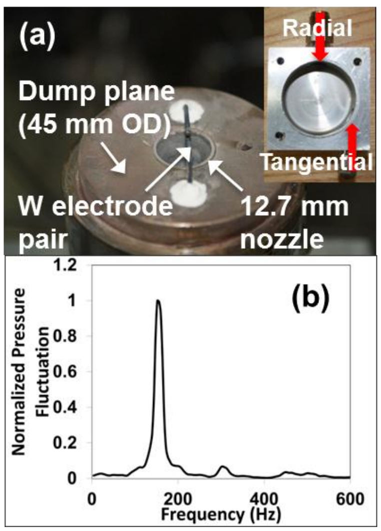

Fig. 1 (a) Photographs of dump combustor and vortex valve (top right); (b) typical uncontrolled pressure oscillation spectrum from the combustor.

A photograph of the premixed dump combustor is presented in Fig. 1a. The combustor consists of a 12.7 mm OD straight tube through which premixed room temperature methane/air is supplied by a variable swirl vortex valve, and a 45 mm OD circular dump volume confined by a ~ 915 mm long open-ended quartz tube. The vortex valve depicted in the sub-picture of Fig. 1a alters swirl strength by varying the split ratio between tangential and radial inlets. The typical chemical power generated by the combustor was ~ 6 kW. Inlet bulk velocity was fixed at ~25 m/s.

Blunted thoriated tungsten electrodes were mounted ~ 3 mm downstream from the dump plane with ~ 1.2 mm gap, and were connected with the NSPD generator. The typical operating conditions of the generator were ~ 7.5kV p-p voltage, 15 – 30 kHz repetition rate (RR), and 15 ns pulse width. The NSPD RR was externally triggered by a delay generator.

Instrumentation included a probe microphone flush-mounted to the dump plane of the burner, pressure signal analyzer, a high speed voltage probe and a Rogowski coil, a spectrometer, a high speed camera, and gas emission sampling equipment for NO_X, CO, CO_2, O_2 measurements. Sampling was conducted using a single tip water cooled probe and the sampling location was ~ 230 mm above the dump plane on the centerline of the quartz tube.

A typical (normalized) pressure fluctuation spectrum is presented in Fig. 1b and was obtained without the NSPD at an equivalence ratio (ϕ) of 0.95 without swirl. Distinct high magnitude peaks were observed in the vicinity of 150 Hz and at its second harmonic, as well as broadband noise from ~ 430 – 530 Hz region. Absolute peak pressure fluctuation levels were ~ O(10^4) Pa, which are consistent with realistic pressure fluctuation levels and frequency profiles of aero-engine combustors. More detailed spectra and their interpretations will be shown in the Section 3.1.

3. Results

3.1. Dynamics reduction

Time-averaged images of flame emission without (left) and with (right) the NSPD for $\phi = 0.9$ and no swirl are presented in Fig. 2. Without the NSPD, the visual length of the flame is ~ 150 mm and the flamebase appears to be stabilized at the outer recirculation zone (ORZ) of the dump plane and is vigorously fluctuating. In the presence of the NSPD, however, the flame was securely anchored to the center zone (CZ), where the NSPD was located, with minimal visible fluctuations. The flame length was also significantly shorter (~ 90 mm) and the observed noise level was dramatically reduced

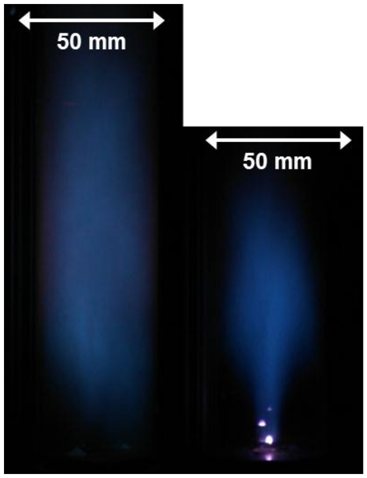

Fig. 2 Flame chemiluminescence images in the absence (left) and presence (right) of the 7.5 kV p-p, 25 kHz RR, NSPD (ϕ=0.9, SN=0)

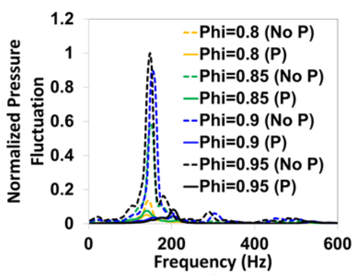

Fig. 3 Reduction of noise level in the absence (dashed) and presence (solid) of the NSPD. The discharge and flame conditions are identical with that of Fig. 2

As a quantification of the sound noise level difference in the presence/absence of the NSPD, the normalized pressure fluctuation spectra with varying equivalence ratio in the absence (dashed) and presence (solid) of NSPD are shown in Fig. 3. The NSPD conditions were identical with those of the previous figure. For all cases investigated, consistently dramatic reduction of dynamics was observed in the presence of the NSPD. For example, the ϕ = 0.95 case showed ~ 25 dB reduction at the peak as well as the elimination of the second harmonic and the broadband noise near the 300 Hz and the 430 – 530 Hz region. During this test, we observed that flames residing further axially downstream from the dump plane tend to exhibit lower dynamics. It is expected that these downstream locations will have less interaction with the vortex shedding region in the vicinity of dump plane, resulting in lower combustion dynamics. This suggests that flame shape and location are critical to understanding and interpreting how the NSPD can dramatically reduce dynamic pressure fluctuation. The detailed investigation of the hypothesized mechanism will be the theme of the following section.

3.2. Dynamics reduction mechanism

Unfiltered flame chemiluminescence high speed images (10 kHz frame-rate) obtained in the absence (left two) and presence (right two) of the NSPD at opposite phase are presented in Fig. 4a. One can find that continuous extinction/re-ignition occurs at each phase without the NSPD while the flamebase and downstream burn more steadily in the presence of the discharge. Simultaneous quantitative time-series data of pressure (p') and spatially integrated flame chemiluminescence (q') fluctuations are presented in Figs. 4b and c with (black) and without (red) the NSPD. The significantly smaller amplitudes for both p' and q' observed with the NSPD indicate that the flame burns much steadier in the time domain likely by spatially decoupling the burning process from fluid unsteadiness such as vortex shedding.

Based on these observations, the hypothesis for noise reduction mechanism with the NSPD is depicted in Fig. 5. The current dump combustor, with similarities to more complex gas turbine combustor geometries, is composed of two zones: a center-zone (CZ) which is relatively steady for the conditions tested, and an outer recirculation zone (ORZ) that is highly affected by fluid unsteadiness. Without the NSPD, the flame is primarily stabilized in the ORZ. Fluid unsteadiness, coupled with combustor acoustics is amplified by the flame in a feedback loop that leads to limit-cycle oscillations with high unsteady pressures. The unsteady fluid mechanics in the ORZ are then exacerbated in this process and cause more unstable, less efficient combustion. In the presence of the NSPD, however, a flame is stabilized in the CZ where the fluid mechanics are steadier and more robust to fluid-acoustic coupling. Unlike previous efforts to control flame dynamics, the current NSPD application is essentially relocating the flame stabilization to break the link between the fluid mechanic fluctuation and flame oscillation.

For a validation of the proposed mechanism, we surveyed the normalized rms pressure fluctuations with varying ϕ as a function of plasma repetition rate (approximately proportional to plasma power) as shown in Fig. 6. Overall, no significant oscillation was detected at ϕ = 0.8 (yellow), therefore, applying NSPD showed no benefit. The visible flamebase location without the NSPD was ~ 100 mm downstream. With an increase of equivalence ratio to 0.85 (green), the flame was pulled upstream and started to reside near the ORZ. The flamebase fluctuation became visibly apparent without the NSPD, and the combustor became thermo-acoustically excited. When the NSPD was turned on and scanned to ~ 24 kHz RR, flame stabilized on the NSPD located at the CZ and sudden noise reduction was achieved. A similar propensity was observed for the ϕ = 0.9 case but its crossover RR was reduced to 22 kHz. At ϕ = 0.95, an interesting "bucket" shape was observed, i.e., the combustor was quiet only when the RR was between 20 kHz to 24 kHz. Outside of the bucket, the plasma power was either too weak (<20 kHz) to relocated the flame from the ORZ to the CZ, or excessively high (>24 kHz) such that the overly "energized" flame shifted upstream and started to reside/fluctuate in the ORZ. In all cases tested, the significant noise reduction was observed only when the flame had the shape confined in the CZ, and any deviation from the shape aggravated the noise. These observations

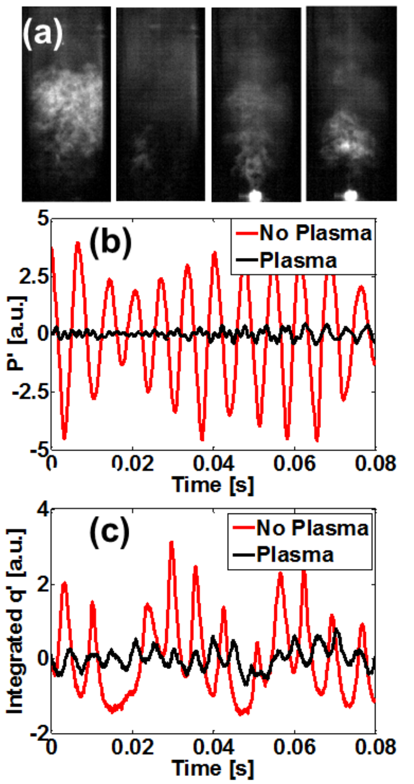

Fig. 4 (a) Unfiltered, 10 kHz frame-rate flame chemiluminescence images at opposite phase in the absence (left two) and presence (right two) of the NSPD, corresponding (b) pressure fluctuation, and (c) spatially averaged chemiluminescence fluctuation time-series

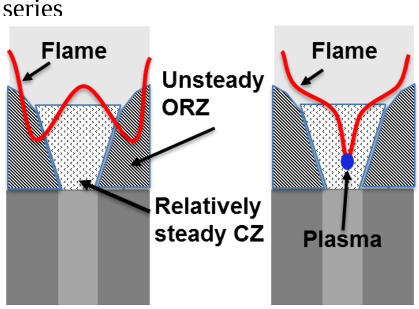

Fig. 5 Schematics of flame shapes without (left) and with (right) plasma

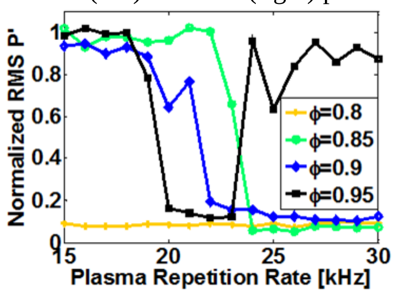

Fig. 6 Normalized p' as a function of plasma RR with varying ϕ

align well with our proposed mechanism depicted in Fig. 5, and further investigation about the combustor noise dependency on the flame shape will be discussed in Section 3.5.

While the authority and mechanism of the NSPD for controlling the combustor dynamics were successfully demonstrated thus far, other important measures of combustor performance, NO_X production and combustion efficiency, will be the topic of the following section.

3.3. Emission and combustion efficiency

Figures 7a and b show incremental $EINO_X$, where $EINO_X$ is defined as grams of NO_X produced per kg fuel consumption, and combustion efficiency (η, calculated based on excess O_2) in the presence of the NSPD with varying RR and applied voltage amplitude. Although it is clear that the NO_X production is a linearly increasing function with the applied voltage and plasma RR, the $EINO_X$ increase was minimal and around ~ 0.5 EI for the typical range of NSPD used in the current study (red circle). The incremental NO_X is due to a combined effect of increasing temperature associated with increasing η and plasma induced NO_X. Surprisingly, the η was not a strong function of the RR and voltage, but its increase in comparison with no NSPD case was consistently significant (~ 10%). According to a separate optical emission spectral analysis for the nitrogen second positive system, the time-averaged rotational temperature (equal to translational temperature at ambient pressure) was 1100 ± 50 K while the vibrational temperature was over 4500 ±100 K, which implies that the plasma is too cold to produce significant level of NO_X, but reactive enough to relocate a flame.

Thus far, we discussed that i) the combustor dynamics is a function of plasma RR or approximately plasma power, ii) produced NO_X is linearly increasing function with the RR, and iii) η is a weak function of the RR. These three ideas are the basis of the newly proposed active control scheme, based on control of plasma power, shown in the following section.

3.4. Plasma power-based active control

Conventional phase-based dynamics control schemes utilize pressure/heat release fluctuation measurements from the combustor and an appropriately selected frequency to eliminate dynamics through destructive interference. There are, however, intrinsic drawbacks of this method such as the inevitable actuator and convective delays that translate to complex spatial phase relations. These delays make complete control challenging. The power-based control proposed here does not require knowledge of the phase. Instead, the flame stabilization point is relocated to an appropriate region (CZ) to avoid thermo-acoustic coupling in the first place.

The control objective is to maintain a CZ stabilized flame with minimal power input to avoid high incremental NO_X production, while maintaining high η. The control algorithm was designed to find the crossover RR (pointed by arrows in Fig. 6) that represents a compromise between dynamics reduction and low NOx production. The same amount of noise reduction, ~25 dB shown in Fig. 3, was successfully demonstrated through this algorithm. While the details are not presented here, our Labview based first generation controller continuously monitored rms pressure fluctuation level. Once a high pressure oscillation was detected, it started a rapid sweep in the plasma RR domain. The sweep stopped when the high gradient of the pressure oscillation was detected, and the system stayed in the RR until another high pressure oscillation was detected.

Thus far, all investigations have been performed without swirl. In the next section, the change of plasma effectiveness under swirling flow will be briefly investigated.

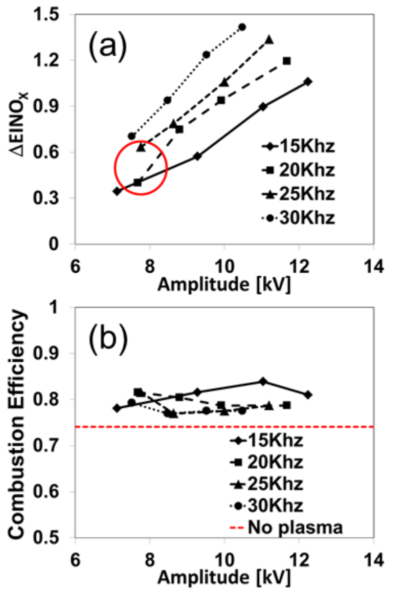

Fig. 7 (a) Incremental $EINO_X$ in the presence of NSPD; (b) Combustion efficiency with (black) and without (red) the NSPD

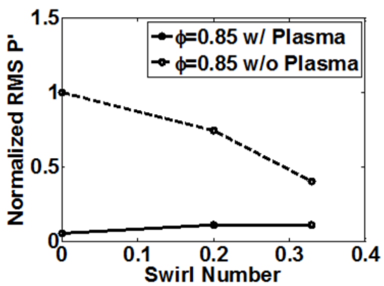

Fig. 8 Normalized rms pressure fluctuation with varying SN

3.5. Swirling flow and flame shape

The introduction of swirl is critical step in moving towards more realistic gas turbine combustor architectures and provides an easy way to change flame shape at fixed flow conditions. In this way, we can validate both the practicality of the current technique and our proposed mechanism, both of which are closely tied to flame shape.

Although not shown here, similar high speed imaging and corresponding p' and q' measurements, as in Fig. 4, were conducted at 0.33 swirl number (SN) in the absence/presence of the NSPD. The 0.33 SN, calculated from separate laser-doppler-velocimetry (LDV) measurements, was chosen because it was close to the maximum swirl number before flashback for the current flow conditions. The swirl numbers utilized in this study reside below the critical level for vortex breakdown. Even without the NSPD, the visible flame length became shorter and the burning appeared steadier in comparison with no swirl case. It was still clear, however, that the flame assisted by the NSPD burned in much steadier manner.

As a quantification, Fig. 8 shows the normalized rms pressure fluctuation with varying swirl in the absence (dashed) and presence (solid) of the NSPD at $\phi = 0.85$. The flame became quieter with increasing swirl even without the NSPD. This decrease in pressure fluctuation is a result of the flame being stabilized near CZ with the increasing swirl, and due to the reduced size of ORZ. As a result, the incremental benefit of NSPD decreases, not as much because plasma loses its effectiveness (the controlled rms pressure does not change appreciably), but because the uncontrolled flame inherently becomes quieter. Although no systematic investigation has been attempted, we observed that even the swirl stabilized flame exhibited higher dynamics when perturbed (e.g., higher velocity) so its flame shape changed to ORZ stabilization. In that situation, the effectiveness of NSPD was more consistent with low swirl conditions, which implies that i) swirl is only one factor in determining flame shape which is a more intrinsic parameter for setting flame robustness to dynamics, and ii) the plasma stabilization effect observed in the current study should still hold for any ORZ stabilized flame shape.

4. Acknowledgement

The material is based upon work supported by NASA under award No. NNX13AB89A.

5. Disclaimer

Any opinions, findings, and conclusions or recommendations expressed in this material are those of the authors and do not necessarily reflect the views of the National Aeronautics and Space Administration.